

Structural, Viscoelastic, and Vulcanization Study of Sponge Ethylene–Propylene–Diene Monomer Composites with Various Carbon Black Loadings

M. Arshad Bashir,¹ Nadeem Iqbal,¹ Mohammad Shahid,¹ Quratulain,¹ Riaz Ahmed²

¹School of Chemical and Material Engineering, National University of Sciences and Technology, Islamabad, Pakistan

²Institute of Industrial Control Systems, P. O. Box 1398, Rawalpindi, Pakistan

Correspondence to: N. Iqbal (E-mail: nadeemiqbal@scme.nust.edu.pk)

ABSTRACT: In this article, we report the effect of various carbon nanoparticle concentrations on the structural, curing, $\tan \delta$, viscosity variation during vulcanization, thermal, and mechanical characteristics of ethylene–propylene–diene monomer polymer sponge composites. The purpose of this study was to develop high-strength, foamy-structure polymer composites with an optimum filler to matrix ratio for advanced engineering applications. We observed that the structural, vulcanization, viscoelastic, and mechanical properties of the fabricated composites were efficiently influenced with the progressive addition of carbon content in the rubber matrix.

© 2013 Wiley Periodicals, Inc. *J. Appl. Polym. Sci.* 000: 000–000, 2013

KEYWORDS: foams; mechanical properties; morphology; rubber; viscosity and viscoelasticity

Received 22 January 2013; accepted 17 April 2013; Published online 00 Month 2013

DOI: 10.1002/app.39423

INTRODUCTION

Polymers exhibit versatility in different ways that differentiate them from other materials, such as ceramics, metals, and their alloys.^{1,2} Sponge or cellular structure elastomeric materials are commercially used for applications where a high impact resistance and buoyancy are required, for example, in gaskets, body armors, and thermal insulation.^{3–5}

The mechanical, thermal, curing, and physical properties of a polymeric material can be engineered by the tuning of its structural characteristics.⁶ These studies have created a new field of research on the large scale for tailoring the properties of polymer composites for diverse applications. The introduction of a gaseous phase in a polymer can be accomplished by the addition of blowing agents that develop a sponge structure within the material.⁷ To enhance the ultimate tensile strength and improve other physical and mechanical properties of polymer composites, various reinforcing agents, such as carbon black, silica, and carbon fiber, can be incorporated into the host matrix.^{8,9}

The reinforcement efficiency needed to tailor the polymer characteristics depends on the concentration, size, and geometry of the impregnated fillers. The addition of carbon black in the polymer matrix imparts a useful influence on the mechanical and curing characteristics, including the curing behavior, scorch safety, and aging properties, of the composite.^{10,11}

Ethylene–propylene–diene monomer (EPDM) sponge is an engineering elastomer having potential applications in damping, thermal insulation, impact resistance, and mechanical strength. EPDM consists of ethylene (45–75%), propylene (13–45%), and diene (2.5–12%). The function of the first monomer is to enhance the loading possibilities of the rubber, the second monomer prevents the polymer from crystallizing, and the last monomer provides active crosslinking sites during vulcanization.^{9,12} Unsaturation is not normally present in the main polymer chain, and because of the presence of the saturated backbone in the polymer, EPDM is more resistant to ozone, oxygen, heat, and UV light. It is useful for outdoor applications, such as sealing systems in buildings, and a few dynamic applications. It is also useful for advanced engineering applications, such as elastomeric ablative composites.^{13,14} EPDM–carbon composites impart better physical and mechanical properties compared to composites reinforced with silica, clay, and so on.¹² Kim et al.¹⁵ studied the mechanical and microstructural properties of sponge composites other than EPDM and established a relationship between the density of the foam cells and the mechanical properties. He concluded that the tensile strength was augmented with carbon black addition in the polymer matrix. The foaming temperature elevation had inverse effects on the density of the fabricated foam and its tensile strength. Viscoelasticity is also a useful property associated with EPDM rubber. These materials exhibit both viscous and elastic

Table I. Base Formulation of the EPDM Rubber Based Foam

EPDM (wt %)	Wax (wt %)	ZnO (wt %)	Stearic acid (wt %)	DPG (wt %)	Sulfur (wt %)	MBTS (wt %)	Aromatic oil (wt %)	Blowing agent (wt %)
100	1	5	1	1	1.5	1	10	5

behavior on deformation.¹⁶ The viscous part associated with the rubber behaves just like honey, as it resists shear flow, and the elastic part shows springlike behavior.¹⁷

The novelty of this investigation resides in the remarkable investigation of the effects of various carbon black concentrations in the presence of a blowing agent on the structural, viscosity variation during curing, $\tan \delta$, and curing rate characteristics of EPDM sponge composites. In this article, we also summarize the influence of the reinforcement loading on the thermal, mechanical, and viscous properties of the sponge rubber composites. These findings will help to optimize the appropriate concentration of carbon black in EPDM foams to develop a better sponge structure with significant thermal, mechanical, and curing characteristics.

EXPERIMENTAL

Materials

Carbon black (N330, 70 nm) was supplied by Continental Carbon. Sulfur, zinc oxide, and stearic acid were supplied by Merck (Germany). Azodicarbonamide, the blowing agent, was provided by Qingdao Xiangsheng (Shandong, China). Mercaptobenzthiazole disulfide (MBTS) and diphenyl guanidine (DPG) were purchased from Dalian Richon Chemical Co., Ltd. (China). Aromatic oil was purchased from International Petrochemicals (Pvt.), Ltd. (Pakistan). EPDM (KELTAN 4331A) rubber was received from Technical Rubber Products (China).

Composition and Fabrication of the EPDM Sponge

Formulation of the EPDM Sponge Composite. Table I elucidates the base formulation schemes of the EPDM sponge rubber composites with various concentrations of carbon black: EF1 (5 wt %), EF2 (10 wt %), EF3 (15 wt %), and EF4 (20 wt %). Sulfur was used as a crosslinker; MBTS and DPG were used as primary and secondary accelerators, respectively. Aromatic oil and wax were used as plasticizers. Zinc oxide and stearic acid were used as activators, and azodicarbonamide was used as a blowing agent to develop a foamy structure in the EPDM composite.

Fabrication of the EPDM Sponge. EPDM rubber was rolled over two-roller mixing mill at 60°C and a 70-rpm roller speed according to ASTM 3182-82 with carbon black (reinforcement), sulfur, zinc oxide/stearic acid, DPG/MBTS, and aromatic oil/wax. The compression produced along the circumferential direction of the rubber bank caused lateral shearing; the rubber bank was cut into a square shape and folded back into the nip repeatedly for uniform dispersion of the constituents within the rubber matrix. EPDM sponge rubber composites were fabricated on a hot isostatic press (Shinto-Japan, 50-ton capacity) at a temperature of 150°C and a pressure of 1 MPa for 20 min. The tensile and rubber hardness testing specimens had dimensions according to ASTM D 412C and D 2240, respectively.

Characterization Techniques

Scanning Electron Microscopy (SEM). The morphology of the sponge EPDM nanocomposites was studied with a scanning electron microscope. The samples were first sputtered with gold to make them conducting, and the cross sections of the samples were analyzed at different magnifications with a JEOL JSM-6490A instrument at 15 kV.

Curing Characteristics. The curing characteristics were determined with a Rheo Check Profile-MD (Gibitre Instruments S. R. L., Italy) according to ASTM 6204 to investigate the various carbon concentrations effects on the lowest or initial torque (M_L), highest or maximum torque (M_H), curing behavior, and $\tan \delta$ values of the uncured polymer composites. The temperature of the upper and lower plates was $190 \pm 0.5^\circ\text{C}$ with an oscillation angle of 0.5° , and the test duration was 3 min.

Thermal Oxidation and Differential Thermal Analyses. A PerkinElmer Diamond thermogravimetric/differential thermal analysis instrument was used to analyze the thermal decomposition and heat flow response of the sponge rubber composites within the temperature range 25–830°C in an air environment with a temperature elevation rate of $10^\circ\text{C}/\text{min}$.

Mechanical Properties. Dumbbell-shaped samples were fabricated according to ASTM D 412 C to characterize the tensile properties of the polymer composites. The ultimate tensile strength, maximum strain, and percentage elongation at break were executed for the each sample of diverse composite formulation with a Tensor Check Profile from Gibitre Instruments S. R. L. All of the tests were carried out at a speed of 500 mm/min. The rubber hardness of the rubber composite specimens was measured with a Shore A durometer according to ASTM D 2240.

RESULTS AND DISCUSSION

Sponge Characteristics

The effects of the carbon black content on the structure and foaming efficiency of the rubber composites is depicted in Figure 1. The SEM images reveal that the spongy structure was a mixture of open and closed cells. The addition of nanocarbon enhanced the elastic behavior and reduced the viscous part of the composite viscoelastic material; this resulted in the reduction of the flowability of the material. So, we observed that the cell sizes and foaming efficiency decreased with increasing carbon content in the rubber matrix from EF1 to EF4. The morphological analysis with SEM at different magnifications of the various nanocarbon-loaded EPDM composites showed that with increasing carbon content in the rubber matrix, the cell size of the foam also decreased synchronously. Another observation over the SEM micrographs was that with increasing filler-to-matrix ratio, the microporosity concentration within the

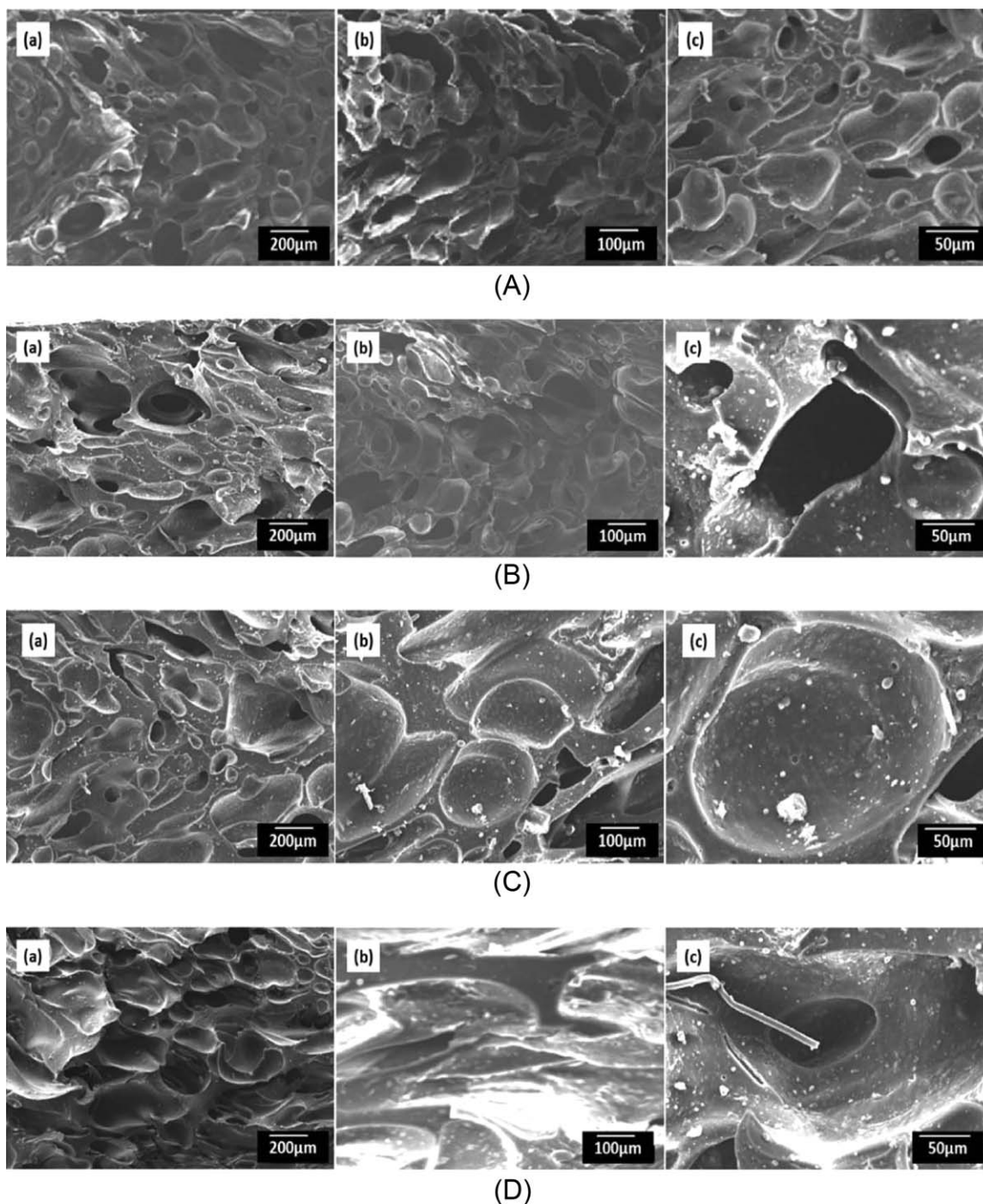


Figure 1. SEM micrographs of the sponge EPDM composites with (A) 5, (B) 10, (C) 15, and (D) 20 wt % carbon contents.

composite decreased gradually because of the crosslinking density enhancement and reduction in bubble formation during the vulcanization of the composites. The number of cells per unit volume was calculated from the SEM images. We observed that with increasing carbon content in the rubber matrix, the amount of generated cells also diminished. The number of cells per unit volume for EF1, EF2, EF3, and EF4 were measured as 500, 380, 200, and 130 cells/mm³, respectively. The carbon acted as a filler and caused rigidity of the base polymer and retarded

the growth of cells by decreasing the viscous part of the base polymer; as a consequence, the number of cells and the cell size decreased. This resulted in the reduction of the foaming efficiency of the fabricated sponge composite specimen.

Curing Characteristics

The curing characteristics of the sponge EPDM with various carbon contents are shown in Figures 2–5. With increasing crosslink density and viscosity of the composite specimens with

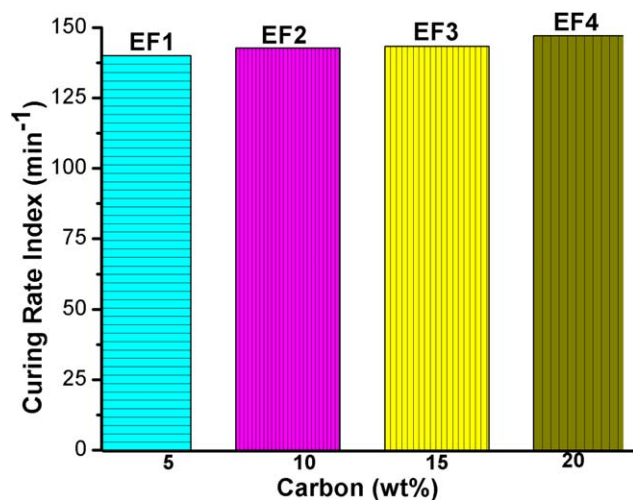


Figure 2. Effect of the carbon black contents on the CRI values of the composite specimens. [Color figure can be viewed in the online issue, which is available at wileyonlinelibrary.com.]

nanocarbon incorporation into the polymer matrix, the rate of vulcanization also accelerated because of the enhancement in vulcanizing sites in the presence of other ingredients, as is clear from Figure 2. This effect is also known as the cure rate index (CRI) and is calculated with the following relationship:

$$\text{CRI} = 100 / (t_{90} - t_{s2}) \quad (1)$$

where t_{90} is the final vulcanization time and t_{s2} is the scorch time of the samples, as elaborated in Figure 3. The scorch time (t_{s2}) is the time for the premature vulcanization of the polymer up to 2%,¹⁸ and t_{s1} is the time between the closure of the dies and the increase in torque up to 1 dN m. Figure 3 also shows a descending trend of the scorch time with increasing carbon black concentration in the EPDM rubber due to viscosity elevation of the composite specimen.¹⁹

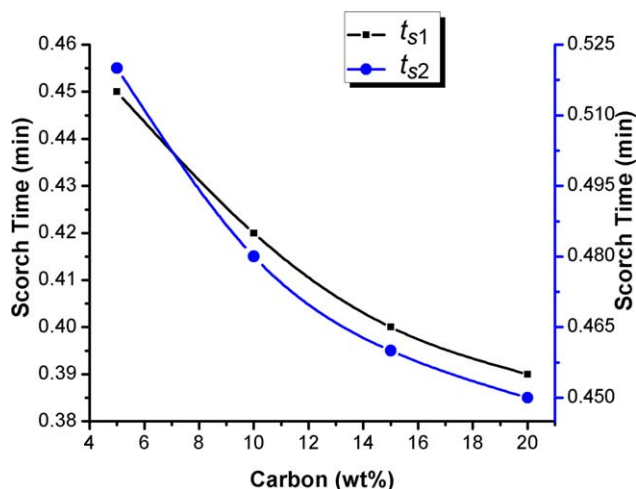


Figure 3. Effect of the carbon black content on the scorch time of the sponge EPDM. [Color figure can be viewed in the online issue, which is available at wileyonlinelibrary.com.]

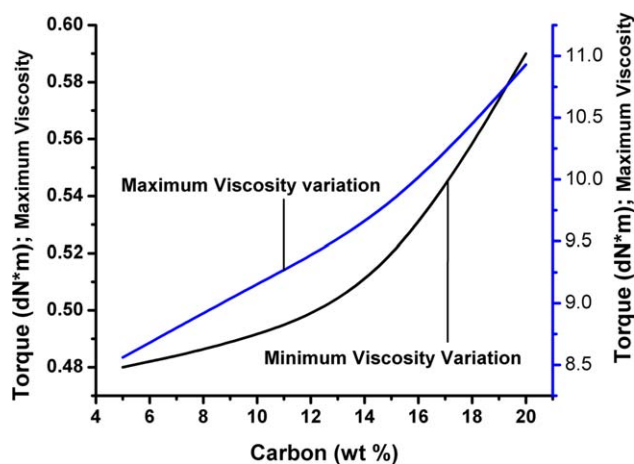


Figure 4. Effect of the carbon black content on the M_H and M_L values of the sponge EPDM composites. [Color figure can be viewed in the online issue, which is available at wileyonlinelibrary.com.]

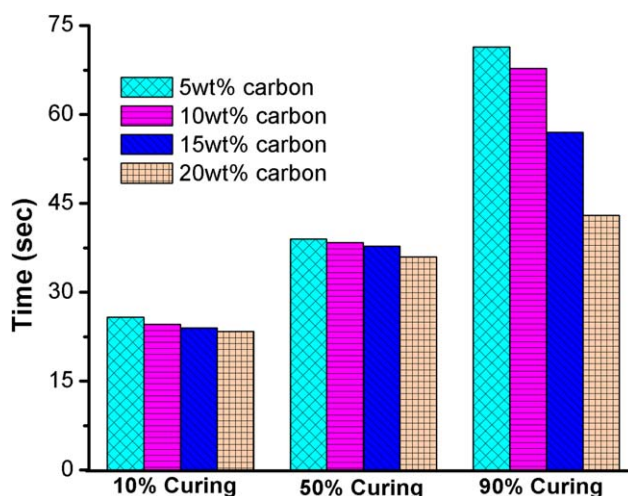


Figure 5. Effect of the carbon black content on the percentage curing with time at 190°C in the sponge EPDM composites. [Color figure can be viewed in the online issue, which is available at wileyonlinelibrary.com.]

Table II elucidates the effect of various concentrations of carbon black on the torque variation of the composite specimens. M_H was related to the crosslink density; this indicated stiffness and shear modulus in the fully vulcanized material. M_L showed the viscosity at the initiation stage of rubber vulcanization.^{7,12,20} The experimental data indicated that the M_H and M_L values increased with increasing carbon contents in the polymer matrix. However, elevation in M_H was more pronounced

Table II. M_H and M_L Variation in the EPDM Sponge Composites with Various Carbon Contents

Property	EF1	EF2	EF3	EF4
M_H (dNm)	8.56	9.16	9.72	10.93
M_L (dNm)	0.48	0.49	0.51	0.59

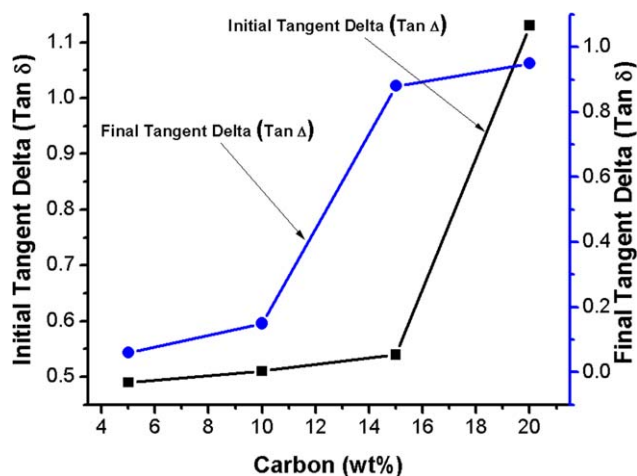


Figure 6. Effect of the carbon black content on the initial and final $\tan \delta$ values of the sponge EPDM composites. [Color figure can be viewed in the online issue, which is available at wileyonlinelibrary.com.]

compared with M_L , as is obvious from Table II, because of the crosslinking density enhancement of the fabricated composites. The carbon black particles acted as the major source for improving the crosslinking between the macromolecular chains of the polymer and the crosslinker and resulted in an upsurge of M_H .

Figure 4 elucidates the effect of carbon black on the maximum and minimum viscosity variations and torque values of the sponge EPDM composite. Generally, with increasing viscosity of the material, the torque values during the vulcanization also progressed synchronously.²¹ The first observation over the presented figure was that in both phases, the torque values increased relative to the filler incorporation increase. Because of the addition of filler, the hard segments of the composite also increased, and this consequently decreased the viscosity of the specimen.

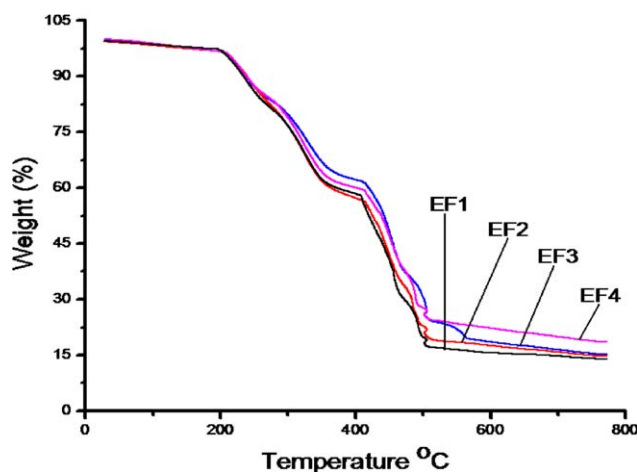


Figure 7. Thermogravimetric analysis of the EPDM sponge rubber composites in an air environment. [Color figure can be viewed in the online issue, which is available at wileyonlinelibrary.com.]

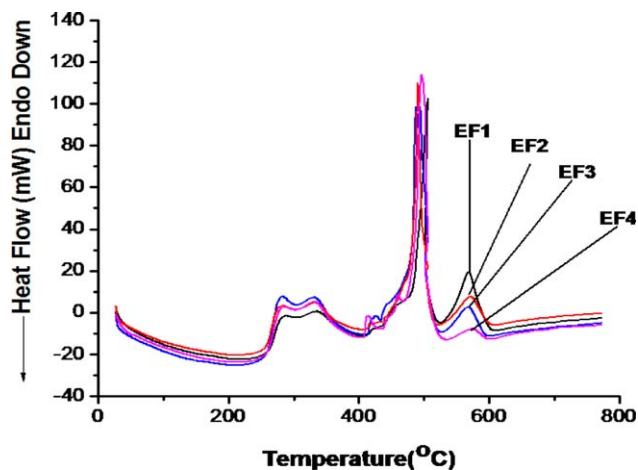


Figure 8. Differential thermal analysis of the EPDM sponge rubber composites. [Color figure can be viewed in the online issue, which is available at wileyonlinelibrary.com.]

The subsequent explanation of this behavior was that with increasing carbon contents, the curing rate also increased. This elevated the crosslink density, and therefore, the viscosity of the composite was augmented accordingly. The phenomenon observed in this experiment was that with the same composite formulation, there were different behaviors of the maximum and minimum viscosity with variation in torque value intensity and rate.^{18,22} We observed that both these parameters were higher for the final variation torque value because of the crosslink density augmentations, which eventually promoted the elastic nature of the composite and decreased the flow of the polymer matrix.

Figure 5 describes the effect of the carbon black contents on the percentage curing with time at 190°C in the sponge EPDM composites. The percentage curing defines the crosslinking efficiency or density of the specimen during the vulcanization process. Low percentage curing of the rubber means a low level of

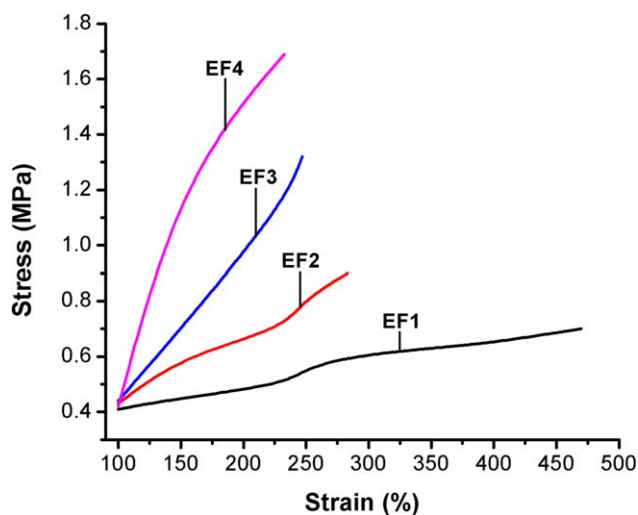


Figure 9. Effect of the nanocarbon concentration on the stress-strain behavior of the fabricated polymer composites. [Color figure can be viewed in the online issue, which is available at wileyonlinelibrary.com.]

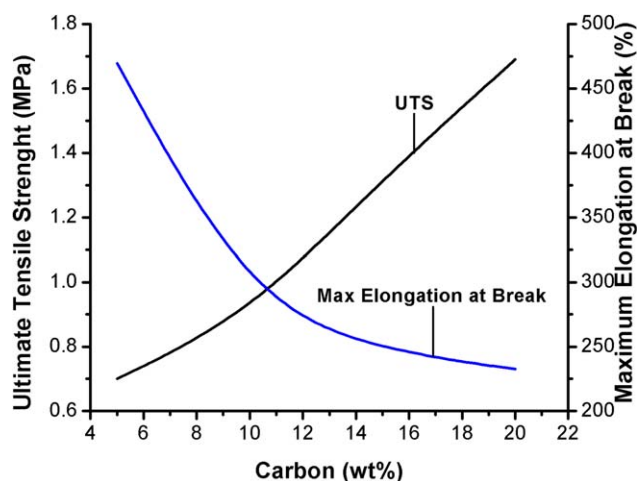


Figure 10. Effect of the carbon black loading on the ultimate tensile strength (UTS) and elongation at break of the EPDM sponge rubber composites. [Color figure can be viewed in the online issue, which is available at wileyonlinelibrary.com.]

crosslink density and vice versa. The times for 10, 50, and 90% curing decreased with increasing carbon concentration in the rubber matrix because of a curing or vulcanization rate enhancement (as observed in the curing study) in which the composites with high carbon contents cured sooner than the other ones. Basically, with increasing carbon concentration in the polymer matrix, heat transport from the source to the polymeric molecular chains also increased, and this endorsed and sped up the vulcanization process.^{10,23–25} Another important parameter deduced from this investigation was $\tan \delta$ (the ratio of the loss modulus to the storage modulus) at the initial ($\leq 10\%$ curing) and final ($\geq 90\%$ curing) vulcanization stages. Figure 6 illustrates the effect of the carbon black contents on the initial and final $\tan \delta$ values of the sponge EPDM composites.^{18,26} Both of the properties of the sponge EPDM composites were improved with increasing carbon content in the rubber matrix. This observation was due to the polymeric chain

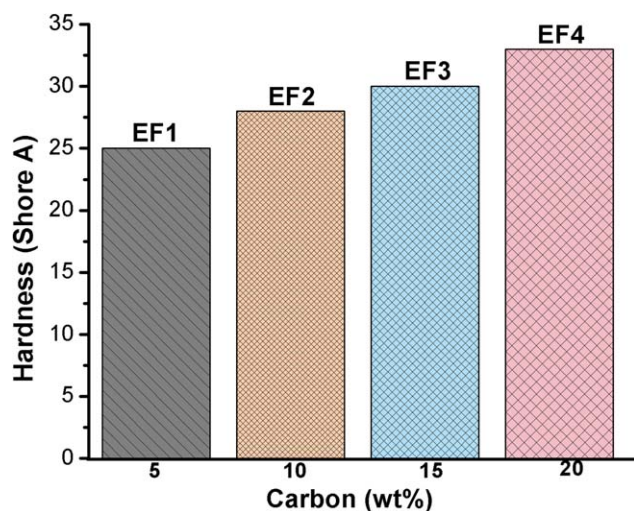


Figure 11. Progress in the EPDM rubber sponge composite hardness with the addition of carbon black in the polymer matrix. [Color figure can be viewed in the online issue, which is available at wileyonlinelibrary.com.]

recovery reduction that occurred because of the heat dissipation enhancement with increasing filler-to-matrix ratio. As a result, the loss modulus increased, and this led to an elevation in $\tan \delta$. This means that with nanocarbon incorporation into the polymer matrix, the viscoelastic nature of the fabricated composites decreased.^{16,27–29}

Thermal Oxidation and Differential Thermal Analyses

Thermogravimetric analysis of the EPDM sponge composites in the temperature range 25–790°C is displayed in Figure 7, which simulates a three-step thermal degradation. The first weight loss could be detected in the temperature range 200–300°C and was due to the evaporation of aromatic oil, wax, and other volatile products. The second major thermal degradation was observed in the temperature range 300–400°C and was due to polymer matrix pyrolysis. The final thermal oxidation was observed in the temperature span 400–500°C and was due to the chain scission of the polymer matrix and the oxidation of the incorporated carbon black.^{30,31}

The incorporation of carbon black in the rubber matrix enhanced the thermal stability of the nanocomposites, as was clear from the presented thermal decomposition response to high thermal endurance compared to the base polymer and nanoscale interaction of the nanocarbon, which restricted the thermal motion of the molecular polymer chains in the heating environment as in Figure 8. We also elucidated that the 6% improvement in thermal stability at 600°C of the composite specimens with increasing nanocarbon concentration in the host matrix.^{4,32}

Mechanical Testing

The effect of various concentrations of carbon black on the mechanical properties of the EPDM sponge rubber composite (tensile strength, elongation at break, and tensile strength at break) are displayed in Figures 9 and 10. The tensile strength and ultimate tensile strength progressed with increasing carbon black content in the rubber matrix, but the elongation at break suffered up to 100% because of the elevation in resistance to flow under pressure or uniaxial force offered by the incorporated nanofiller.²³ A remarkable augmentation up to 240% in the ultimate tensile strength of the sponge rubber composite was observed with the 20 wt % nanocarbon introduction into the polymer matrix as compared to the 5 wt % filled rubber composite.³³ The enhancement in the mechanical aspects was due to the fact that carbon black acted as a reinforcing filler in the composite, and it increased both the crosslinking density and viscosity by occupying active sites of the branched chains of the base polymer by filling up the microvoids existing in it. As a consequence, composite strengthening was achieved. The hardness profile of the sponge also exhibited similar behavior, as is clear from Figure 11. The nanocarbon acted as a filler in the polymer, thereby hardening the material and increasing the deformation resistance of the composite.^{14,17,33} It also reduced the flowing efficiency of the polymeric molecular chains under pressure of force.

CONCLUSIONS

EPDM sponge polymer composites with various nanocarbon loadings were fabricated to scrutinize the progressive filler

incorporation effects on the structural, curing, rheology, thermal, and mechanical properties of the composite specimens. We observed that the cell size and porosity in the fabricated foamy composites were reduced with increasing filler to matrix ratio. The curing rate was enhanced and t_{s1} and t_{s2} decreased with increasing filler concentration in the polymer matrix. The torque values were increased with carbon loading and percentage curing. The thermal stability and endothermic capability of the composite specimens were elevated with increasing filler contents in the polymer matrix. The ultimate tensile strength and rubber hardness progressed up to 240 and 32% with the peak addition of nanocarbon loading in the rubber matrix. Briefly, with increasing carbon contents in the polymer matrix, the viscoelastic and foamy behavior were reduced, whereas the curing and mechanical strength aspects of the sponge EPDM were augmented accordingly in the composite.

ACKNOWLEDGMENTS

The authors gratefully acknowledge the support of the Higher Education Commission of Pakistan for this research.

REFERENCES

1. Moniruzzaman, M.; Winey, K. I. *Macromolecules* **2006**, *39*, 5194.
2. Iqbal, N.; Khan, M. B.; Sagar, S.; Maqsood, A. *J. Appl. Polym. Sci.* **2013**, *128*, 2439.
3. Zhang, C.; Pal, K.; Byeon, J. U.; Han, S. M.; Kim, J. K. *J. Appl. Polym. Sci.* **2011**, *119*, 2737.
4. Li, L. P.; Li, B.; Tang, F. *Eur. Polym. J.* **2007**, *43*, 2604.
5. Bhuvaneswari, C.; Sureshkumar, M.; Kakade, S.; Gupta, M. *Def. Sci. J.* **2006**, *56*, 309.
6. Gao, G.; Zhang, Z.; Li, X.; Meng, Q.; Zheng, Y. *Polym. Bull.* **2009**, *64*, 607.
7. Mahapatra, S. P.; Tripathy, D. K. *J. Appl. Polym. Sci.* **2008**, *109*, 1022.
8. Nair, A. B.; Kurian, P.; Joseph, R. *Mater. Des.* **2012**, *36*, 767.
9. Zhang, B. S.; Lv, X. F.; Zhang, Z. X.; Liu, Y.; Kim, J. K.; Xin, Z. X. *Mater. Des.* **2010**, *31*, 3106.
10. Ghosh, P.; Chakrabarti, A. *Eur. Polym. J.* **2000**, *36*, 607.
11. López Gaxiola, D.; Jubinski, M. M.; Keith, J. M.; King, J. A.; Miskioglu, I. *J. Appl. Polym. Sci.* **2010**, *118*, 1620.
12. Malas, A.; Das, C. K. *J. Mater. Sci.* **2012**, *47*, 2016.
13. Wingard, C. D. *Thermochim. Acta* **2000**, *357*, 303.
14. Natali, M.; Monti, M.; Puglia, D.; Kenny, J. M.; Torre, L. *Compos. A* **2012**, *43*, 174.
15. Kim, E. S.; Kim, E. J.; Lee, T. H.; Yoon, J. S. *J. Appl. Polym. Sci.* **2012**, *125*, E298.
16. Mahapatra, S. P.; Tripathy, D. K. *J. Appl. Polym. Sci.* **2006**, *102*, 1600.
17. Sombatsompop, N. *J. Appl. Polym. Sci.* **1999**, *74*, 1129.
18. Abdel-Aziz, M.; Basfar, A. *Polym. Test.* **2000**, *19*, 591.
19. Wang, B. Q.; Peng, Z. L.; Zhang, Y.; Zhang, Y. X. *J. Appl. Polym. Sci.* **2006**, *101*, 3387.
20. Dijkhuis, K. A. J.; Noordermeer, J. W. M.; Dierkes, W. K. *Eur. Polym. J.* **2009**, *45*, 3302.
21. Lee, E. K.; Choi, S. Y. *Korean J. Chem. Eng.* **2007**, *24*, 1070.
22. Sun, X. H.; Zhang, G.; Shi, Q.; Tang, B.; Wu, Z. W. *J. Appl. Polym. Sci.* **2002**, *86*, 3712.
23. Abdel-Aziz, M.; Basfar, A. *Nucl. Instrum. Methods Phys. Res. Sect. A* **2001**, *185*, 346.
24. Ghassemieh, E. *Polym. Compos.* **2009**, *30*, 1657.
25. Wimolmala, E.; Khongnual, K.; Sombatsompop, N. *J. Appl. Polym. Sci.* **2009**, *114*, 2816.
26. Ghosh, P.; Katare, S.; Patkar, P.; Caruthers, J. M.; Venkatasubramanian, V.; Walker, K. A. *Rubber Chem. Technol.* **2003**, *76*, 592.
27. Sarkhel, G.; Choudhury, A. *J. Appl. Polym. Sci.* **2008**, *108*, 3442.
28. Guriya, K. C.; Tripathy, D. K. *J. Appl. Polym. Sci.* **1998**, *68*, 263.
29. Adohi, B. J. P.; Mdarhri, A.; Prunier, C.; Haidar, B.; Brosseau, C. *J. Appl. Phys.* **2010**, *108*, 074108.
30. Rajeev, R.; De, S.; Bhowmick, A. K.; John, B. *Polym. Degrad. Stab.* **2003**, *79*, 449.
31. Basfar, A.; Abdel-Aziz, M.; Mofti, S. *Polym. Degrad. Stab.* **1999**, *66*, 191.
32. Desai, A. Ph.D. Dissertation, University of Southern California, **2008**.
33. Vasilakos, S.; Tarantili, P. *J. Appl. Polym. Sci.* **2011**, *125*, E548.